This is a peer-reviewed, author's accepted manuscript of the following research article:
Nematiaram, T. (2020).
On the largest possible mobility of molecular semiconductors and how to achieve it. Advanced Functional Materials, 30(30), [2001906].
https://doi.org/10.1002/adfm.202001906

On the largest possible mobility of molecular semiconductors and how to achieve it

Tahereh Nematiaram[a], Daniele Padula[a,b], Alessandro Landi [a,c], Alessandro Troisi[a,*]

[a]Department of Chemistry and Materials Innovation Factory, University of Liverpool, Liverpool L69 7ZD, U.K.

[b]Dipartimento di Biotecnologie, Chimica e Farmacia, Università di Siena, via A. Moro 2, 53100, Siena, Italy

[c]Dipartimento di Chimica e Biologia, Università di Salerno, I-84084 Fisciano, Salerno, Italy

*a.troisi@liverpool.ac.uk

Abstract

We use a large database of known molecular semiconductors to define a plausible physical limit to the charge carrier mobility achievable within this materials class, and a clear path toward this limit. From a detailed study of the desirable properties in a large dataset, it is possible to establish whether such properties can be optimized independently and what would be a reasonably achievable optimum for each of them, regardless of the transport mechanism considered. We compute all relevant parameters from a set of almost five thousand known molecular semiconductors, finding that the best known materials are not ideal with respect to all properties. These parameters in decreasing order of importance are realized to be the molecular area, the non-local electron-phonon coupling, the two-dimensional nature of transport, the local electron-phonon coupling and the highest transfer integral. We also find that the key properties related to the charge transport are either uncorrelated or 'constructively' correlated (i.e. they improve together) concluding that a ten-fold increase in mobility is within reach in a statistical sense, on the basis of the available data. We demonstrate that high throughput screenings, when coupled with physical models of transport produce not only specific target materials, as it is done also here, but a more general physical understanding of the materials space and the opportunities of further development.

TOC GRAPHICS:

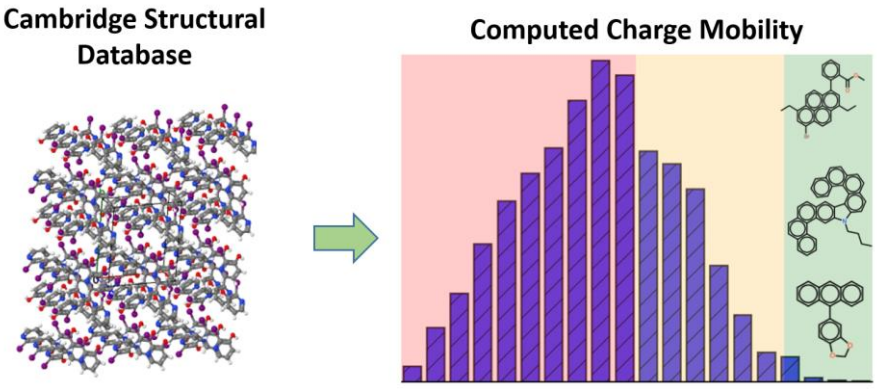

TOC SUMMARY:

We have evaluated the physical parameters relevant for charge transport for ~5,000 known molecular semiconductors extracted from the Cambridge structural database and computed the expected charge mobility. We find a number of potential high mobility semiconductors and, by studying the distribution of such parameters we predict the physical limit to the charge mobility achievable within this materials class.

1. Introduction

Using large databases to discover materials with interesting properties is now one of the main avenues of modern materials chemistry research.[1–4] Quantum mechanical computational models can often provide a sufficiently accurate evaluation of simple properties, such as electronic state energies or binding energies, which in turn have been used to identify stable compositions[5,6] or materials with suitable energy levels for special applications.[7–9] Substantially more challenging is the use of the existing databases to predict complex properties (e.g. charge mobility, superconductivity, thermoelectricity), depending on several material characteristics and the particular choice of the physical model.[10–12] Crucially, one is not only interested in identifying the best hits within a given dataset but in predicting the *achievable* performance of the entire materials class, i.e. how well one can expect to optimize the individual characteristics of the material using the known materials as a source of information on the allowed range for such characteristics. In this work, we aim to combine high throughput calculations and physical models to predict the optimal (hole) mobility achievable by molecular semiconductors, one of their most critical characteristics.[13,14] A critical experimental achievement of the past 15 years has been the measurement of intrinsic charge carrier mobility of molecular crystals.[15] While the measurement of mobility is influenced by the methodology used to extract them, measurement in thin-film transistors are becoming extremely reproducible across different groups.[16] As the measured mobility depends on the purity of crystals[17] and is likely influenced by the degree of polycrystallinity,[18] it is essential to realize that a relation between crystal structure and mobility can be obtained only when single crystal intrinsic (defect free) mobilities are measured. This has now become the standard for reporting materials with record mobility like rubrene, [19], [20], with intrinsic nature of transport verified by comparison with Hall mobility[16,21] or "band-like" temperature dependence.[22] The goal of this paper is to contribute to the discovery of the best materials prepared and measured in these conditions.

From a theoretical point of view, predicting charge mobility for a given material requires two distinct components: the computation of the materials parameters from its structure and the computation of the mobility from such parameters. Although the best theoretical methods used to connect the system parameters to the mobility are still debated,[23–25] there is essentially a consensus on what such parameters are, i.e. on the model Hamiltonian. The hole occupies states on the highest occupied band, which is typically narrower than the inter-band energy and defined by the *transfer integrals* J_{ij} between the HOMO localized on neighbouring molecules. Phonons play different roles depending on their energy $\hbar\omega_M$ (M is the index of the phonon mode). The displacements along a mode Q_M modify the on-site energy by the so-called *local electron-phonon coupling* term $g_M\hbar\omega_M Q_M$.[26] If this term is large enough, the carrier is trapped

in a single molecule and diffuses in the lattice through incoherent hopping mechanism;[25] however, this regime can only be observed for very low mobility.[27] Phonons with a strong role in local electron-phonon coupling are often high frequency modes (600-1700 cm^{-1}) involving stretching and bending of the main conjugated portion of the molecule.[28] The lower frequency modes are instead more active in modifying the transfer integral through the *non-local electron-phonon coupling* $g_{M,ij}\hbar\omega_M Q_M$. Due to the quasi-classical nature of the low frequency modes, the main effect of the non-local electron phonon coupling is to create fluctuations of the transfer integral, which are of the same order of magnitude of the transfer integral itself.[29]

Regardless of the adopted transport model, a material is fully described by a set of transfer integrals and local and non-local electron-phonon coupling: the best materials are expected to have the broadest electronic bands and the smallest electron-phonon coupling.[30–34] The evaluation of electron-phonon coupling is computationally extremely expensive (especially the computation of the phonons of molecular crystals) and has never been considered so far for materials screening or discovery. Existing works report calculations on one[35] or few[36,37] molecules, which, for state of the art calculations, required millions of CPU hours.[28] In this work (section 2) we introduce several approximations that enable the calculation of all the important properties for *thousands* of molecular semiconductors. The two orders of magnitude expansion of the computable landscape allows a complete mapping of all semiconducting molecular materials deposited in the Cambridge Structural Database (CSD) and can be used (section 3.1) to establish the physical range of all parameters contributing to the mobility and their correlation. When such parameters and their distribution are fed into a suitable model for the computation of the mobility (section 3.2) one can identify new high mobility candidates and construct a model for physically achievable maximum mobility.

2. Methodology

Below we outline the overall methodology stressing the components that deviate from similar works published before.[32,38,39] In particular, we highlight in the main manuscript the methods used to accelerate the evaluation of the system parameters with further details and the validation of each approximation given in the Supporting Information (SI).

Dataset. We consider a set of ~40k molecular semiconductors extracted from the million structures in the Cambridge Structural Database[40] as detailed in ref.[7] (the same set is used here). The structures considered are all organic (i.e. containing elements H, B, C, N, O, F, Si, P, S, Cl, As, Se, Br, I) and exclude co-crystals, polymers, disordered solids, duplicate structures and materials containing molecules with more

than 100 atoms. To restrict the study to semiconductors we considered only molecules with computed HOMO-LUMO gap between 2 and 4 eV.

Transfer integral calculations. The transfer integral between HOMO orbitals of two neighbouring molecules is computed based on the algorithm presented in Ref.[41] from the equation $J_{ij} = \langle \varphi_i | \hat{F} | \varphi_j \rangle$, where φ_i and φ_j are the unperturbed HOMO orbitals of the two isolated distinct molecules and $\hat{F}$ is the Fock operator of the dimer system. We computed the transfer integrals between all non-equivalent pairs of molecules in van der Waals contact, e.g. molecules such that at least one distance between any two atoms *i* and *j* is shorter than $1.2\times(r_i + r_j)$ with r_i and r_j being the van der Waals radii from Ref.[42]. Calculations of the transfer integrals are carried out at the B3LYP/3-21g* level of the theory, which shows an extremely large correlation (r=0.997) with calculations using larger basis set (B3LYP/6-311g**), as detailed in the SI (pages 2-3).

Approximated phonons. The calculation of crystal vibrations or phonons is an extremely time consuming process. We significantly speed up the calculations by considering approximated phonons, i.e. assuming that each molecule oscillates independently from the others. We assume that all phonons including those deriving from translation and rotation of the isolated molecules (acoustic and libration modes) are localized on a single molecule (Einstein dispersion-less phonons). We compute them as the vibrational modes of a molecule embedded by the surrounding (rigid) molecules in a Quantum Mechanics/ Molecular Mechanics (QM/MM) calculation.[43] We perform the calculations using the ONIOM scheme (B3LYP/3-21G*:UFF) with embedded charges,[44] as implemented in Gaussian16.[45] As detailed in the SI (pages 6-7), this method leads to results in good agreement with the data obtained from more accurate approaches.

Local electron-phonon coupling. The local electron-phonon coupling g_M is computed using the nuclear displacements between equilibrium positions of neutral and +1 charged molecule projected on the molecular vibrational modes as detailed in ref.[46].

Non-local electron-phonon coupling. In order to shorten the computational time while providing reliable results, we have approximated the derivative of the transfer integrals as $\{fJ/fq_i\} \cup J/S\{fS/fq_i\}$ where *J* and *S* are respectively the transfer integral and overlap at equilibrium geometries and q_i denote Cartesian coordinates of atoms. Furthermore, the component of the gradient along the coordinates of the hydrogen atoms (H) is neglected as the frontier orbital have π character, therefore, they are not affected significantly by displacement of H where the orbital wavefunction has no population. In the SI (page 6) we show that the cumulative effect of these approximations on the gradient of the transfer integral is

negligible. As such, the correlation coefficient between approximated and non-approximated gradient of transfer integrals is 0.9882.

Mobility calculation. Transient localization theory[23,47] is used to evaluate the mobility as it produces results in agreement with more complicated quantum dynamics propagation schemes[33,48] while being sufficiently fast to be employed for thousands of different problems. According to transient localization theory, the effects of the dynamic disorder can be monitored by a transient localization over a length L within a fluctuation time τ. We use the exact diagonalization method proposed in ref.[49] to calculate the squared transient localization length in crystal's high mobility plane. Furthermore, we have also modified the original theory to incorporate the impact of local electron-phonon coupling in addition to non-local electron-phonon term. As such an additional on-site Gaussian fluctuation σ_{local} is considered which takes into account the impact of high-frequency modes and the transfer integrals and their fluctuations are scaled by the renormalization factor f which considers the low-frequency vibrations (see SI (pages 8-9) for further detail).

Validation of the overall approach. This method has demonstrated the ability to correctly predicts the charge mobility of a range of materials for which single crystal thin-film transistor have been measured and, so far, 13 different high-mobility materials have been studied between ref.[32] and ref.[28]. In all these studies the bulk crystal structure at room temperature was used to compute the mobility in the high-mobility plane. The agreement implies that the small possible differences in thin-film geometries with respect to the bulk are not sufficient to alter the relative mobility of the materials and one can perform useful predictions from the crystal structure. Furthermore, in the cases considered so far, the high mobility plane is, without any known exception, the plane in contact with the gate insulator in thin-film transistor geometry. In essence, provided that materials could be grown as single crystals in a highly purified form there is a reassuringly good degree of agreement between different theoretical models for the mobility[33,50] and between them and intrinsic mobility measurements.[32,38]

3. Results

3.1 Overview of the electronic properties of the database

We have evaluated the transfer integrals between HOMO orbitals in symmetry independent molecular pairs at Van der Waals contact. This calculation, in effect equivalent to computing the band structure of the whole set, was used to screen out materials that are unlikely to be good semiconductors. The results of electronic structure calculations alone enable interesting insights on issues broadly discussed in the literature but never addressed with a statistically very large sample of materials.

To collect the results in a convenient way, to each transfer integral we associate a vector *R* connecting the centre of mass of the molecules involved in the coupling. We denote with J_1 the *largest transfer integral* in absolute value and with J_2 the second largest transfer integral in absolute value whose corresponding R_2 is non-parallel to R_1. It has been long observed that the high mobility semiconductors have a high-mobility plane with poor delocalization and transport in the direction perpendicular to this plane,[51] thus, many theoretical investigations focus on transport in two-dimensions.[32,33,52] In this study, we assume that the plane constructed by these two vectors is the plane of high mobility and all the relevant calculations for mobility are performed on pairs lying in this plane. We define the parameter $2D = |J_2|/|J_1|$ to describe materials that are predominantly one-dimensional, with $2D$ close to 0, or have more isotropic bands in two dimensions, with $2D$ close to 1.

An interesting question which can be answered based on these data is how often one could find one- or three- dimensional bands. The results analysis indicates that 8% of the structures are predominately one-dimensional, i.e. $2D \leq 0.05$, (an undesirable property regardless of the transport mechanism[32,53]). Moreover, we find that 1.93% of the structures possess bands extending in three dimensions, i.e. with a transfer integral outside the plane defined by J_1 and J_2 greater than $0.5 \times |J_2|$. However, the majority of these structures possess small transfer integrals and only 6 materials have relatively broad three dimensional bands with $|J_1| \geq 0.1$ eV (these structures are listed in the SI, page 14). We conclude that developing charge transport models working in two dimensions is both necessary and sufficient for screening a large set of materials.

Our results also give a global picture of relative energies distributions, as such, the median of computed HOMO and LUMO energy levels are respectively -5.44 eV and -1.92 eV with an interquartile distance of 0.73 and 0.83 eV, respectively. Moreover, the median energy separation between HOMO and HOMO-1 energy levels is 0.66 eV. Considering the fact that the transfer integral $|J_1|$ is never greater than 0.4 eV and its median is 0.14 eV (see its distribution in the next section), one can conclude that the band energies do not overlap effectively and, therefore, the approximation that the valence band originates solely from the HOMO orbital is generally valid.

3.2 Distribution of properties contributing to the mobility

The additional properties that contribute to the mobility require the evaluation of the electron-phonon coupling, a very expensive calculation that is conveniently performed only for the most promising structures. As such, we consider further only materials with $|J_1| \geq 0.1$ eV, to avoid considering materials with an overall too narrow band-width and $2D \geq 0.05$ to exclude materials whose transport is

predominantly one-dimensional. These criteria define a reduced set of 4801 materials, further considered for an in-depth study of the electron-phonon coupling and the mobility. Figure 1 collects the distribution for some parameters relevant to transport, to be correlated with computed mobility that are further described below.

Non-local electron-phonon coupling. To condense the information of the non-local electron-phonon coupling into few parameters one can compute the fluctuations of the individual transfer integrals at room temperature σ_{ij} or define a weighted average of the *relative* fluctuations of the two strongest couplings as $\alpha = \frac{J_1^2}{J_1^2+J_2^2}\left(\frac{s_1}{J_1}\right) + \frac{J_2^2}{J_1^2+J_2^2}\left(\frac{s_2}{J_2}\right)$. Figure 1 illustrates the distribution of this quantity which is peaked around 0.5, the value seen in many evaluations in the literature,[32] but with a significant number of materials displaying very small (and therefore promising) $\alpha < 0.2$. Since the high mobility of the best molecular semiconductors has been often explained by a particularly small non-local electron-phonon coupling,[34,54] the identification of the smallest 'realistic' α offers a natural achievable target for materials design. The relative disorder α is related but not identical to the parameter σ/J defined in ref.[34] but the conclusion are unaffected by the choice made.

Local electron-phonon coupling. The local electron-phonon coupling, has different roles at low- and high-phonon frequency. Coupling with high frequency modes in high mobility semiconductor causes a renormalization (reduction) of the transfer integral by a factor *f*.[55] The effect of coupling with low frequency modes is instead better seen as causing a fluctuation of the on-site energy σ_{local}. To characterize both effects we have defined the boundary between "low" and "high" frequency nuclear modes as $2k_BT$ at T=290 K, computed *f* and σ_{local}, and reported the distribution of these values in Figure 1(d-e).

An interesting question which can be addressed based on this data is whether, as often assumed in the literature, the local and non-local electron-phonon couplings are dominated respectively by high- and low-frequency modes. Our finding reveals that the median of high energy modes contribution to the local and non-local types of couplings is respectively 84% and 25% (see SI pages 3-4). This implies that neither all the phonons contributing to local electron-phonon coupling are high energy nor the ones affecting the non-local electron-phonon couplings are fully classical (low energy) phonons. This broad range of distribution of frequencies is usually neglected in theoretical models and is highly relevant for the development of charge transport theories. For instance, the semiclassical quantum dynamics assume that

nuclear motions are all classical[56] and renormalization theories are designed for high-frequency (quantum) phonons.[55]

Molecular area. The area per molecule (unit cell area divided by the number of molecules) in the high mobility plane A_m is important, because, as it is shown for instance in ref.[32], the mobility is proportional to the square of the lattice spacing and, if one could deform the 2D lattice keeping all the other parameters constant, the average mobility in the plane would be proportional to the area per molecule. According to Figure 1, the distribution of molecular area is very broad, such that, the inter-quartile distance is larger than the median value. Despite the trivial role of the molecular area, analysing the available geometries reveals that this parameter can be considered as a potential target for optimization.

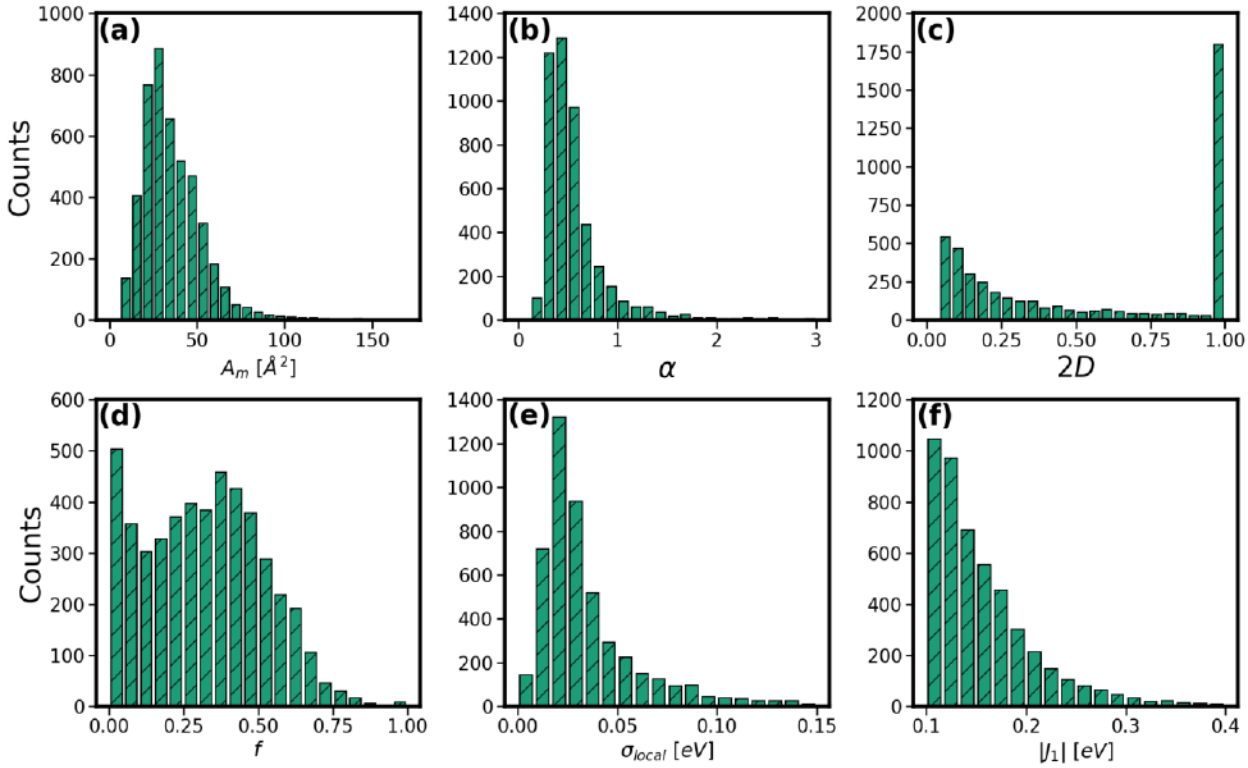

Figure 1. (a-f) Distribution of the main parameters influencing the mobility: the area per molecule (A_m), the relative non-local electron-phonon coupling (α), the 2-dimensionality of transport (*2D*), the band renormalization due to local electron-phonon coupling (*f*), the fluctuation of the on-site energy due to low frequency modes (σ_{local}) and the absolute value of highest transfer integral ($|J_1|$).

Correlation between parameters. The existence of correlation (or anticorrelation) between the materials characteristic parameters that contribute to the mobility can facilitate (or prevent) their concurrent optimization. Therefore, a key question is to determine whether it is possible to optimize the materials

further, i.e. if it is feasible to improve *independently* the desirable characteristics. Accordingly, in Figure 2, the correlation matrix between the six key parameters entering in any mobility theory (i.e. A_m, α, $2D$, f, σ_{local} and J_1) plus the inverse effective mass $1/m^*$ (computed from band structure and included as it is the most relevant electronic parameter used in the band theory) are evaluated. Since $1/m^*$ increases with area and J_1, as expected from its definition, the correlations of $1/m^*$ with any other parameter are intermediate between those of A_m and J_1, so they do not need to be discussed in detail. Therefore, the only remarkable correlations (i.e. in absolute value greater than 0.2) left are, (i) σ_{local} and f, i.e. the electron-phonon coupling with high- and low- frequency modes grow/decrease together. (ii) α and J_1 are negatively correlated, partially due to the definition of α as weighted relative disorder. This correlation is inconsequential given the very small correlation between J_1 and the mobility. Therefore, one can conclude that the 6 key quantities related to the mobility display a marginal level of correlation, i.e. they can be optimized separately.

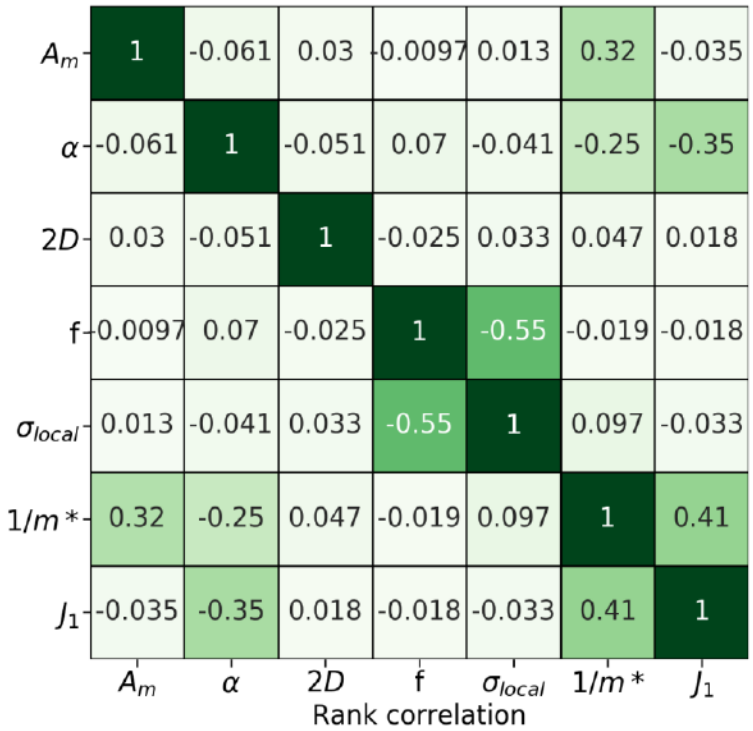

Figure 2. Correlation matrix reflecting the rank correlation between the various parameters affecting the mobility.

Before discussing the effects of the materials parameters on the computed mobility it is important to stress that all the findings outlined so far are independent of the specific transport model adopted and provide important guidance for the design of materials, identification of plausible target properties and development of the best approximations for theoretical models. For example, we have found that:

(i) The band generated by the molecular HOMO is sufficient to describe the hole wavefunction.

(ii) The vast majority of the materials form $2D$ bands but, if one request at least a moderate bandwidth, only 12% of semiconducting materials are worth considering in detail.

(iii) The distribution of area per molecule is so broad that it can become a target for material design.

(iv) One of the generally accepted limiting factor for the mobility, the non-local electron-phonon coupling, is very broadly distributed and it can become much smaller than what it is in the best currently available materials.

(v) The parameters contributing to the mobility are largely uncorrelated.

(vi) Both high and low-frequency phonons contribute to both local and non-local electron-phonon coupling suggesting a clear area of required improvement in many current theories.

These findings exemplify very nicely how a new body of knowledge, superior to the intuitive collection of information from many different sources, can be obtained from a high throughput study of realistic materials.

3.3 Correlation with computed mobility

The next step is to evaluate the mobility for the data set and study the role of each component and the maximum mobility realistically achievable within this class of materials. The calculation is performed for the highest mobility plane in the framework of transient localization theory; the distribution of the computed mobilities μ (averaged in the plane) is presented in Figure 3(a). We have divided the materials into "Group A" with $\mu < 1$ cm^2/Vs (~3300 structures), "Group B" μ in the interval [1 – 6] cm^2/Vs (~1400 structures) and "Group C" with $\mu > 6$ cm^2/Vs (40 structures with largest mobility 13 cm^2/Vs).

Interesting design principles can be drawn from the degree of correlation between the computed mobilities and system's parameters. This is practical because the parameters are either uncorrelated or constructively correlated as explained previously. Accordingly, in Figure 3(b), the rank correlation between mobility and the system's parameters considering (first row) the entire database {ABC}, (second row) only materials displaying mobilities larger than 1 cm^2/Vs {BC} and (third row) the top 40 molecules {C} is shown. One can immediately see that large area per molecule, small non-local electron-phonon coupling and higher $2D$ parameters are correlated with higher mobilities. A smaller but non-negligible correlation is seen with the band renormalization parameter f and the on-site local fluctuations σ_{local}. As can be seen, the correlation is larger if computed only for higher mobility material, i.e. groups B and C or group C only. This behaviour is consistent with the variation range of parameters among group A, B and C materials as shown in the bottom panels in a series of "box plots". A parameter that, maybe surprisingly, is marginally

correlated with the mobility than these five is $|J_1|$, a fact in contrast with hopping models[11] but expected for high mobility materials.[32] This is partly inherent to transient localization theory but, on a qualitative level, the poor correlation between $|J_1|$ and mobility derives from the electronic structure data: larger transfer integrals are invariably associated with larger *absolute* electron-phonon coupling.

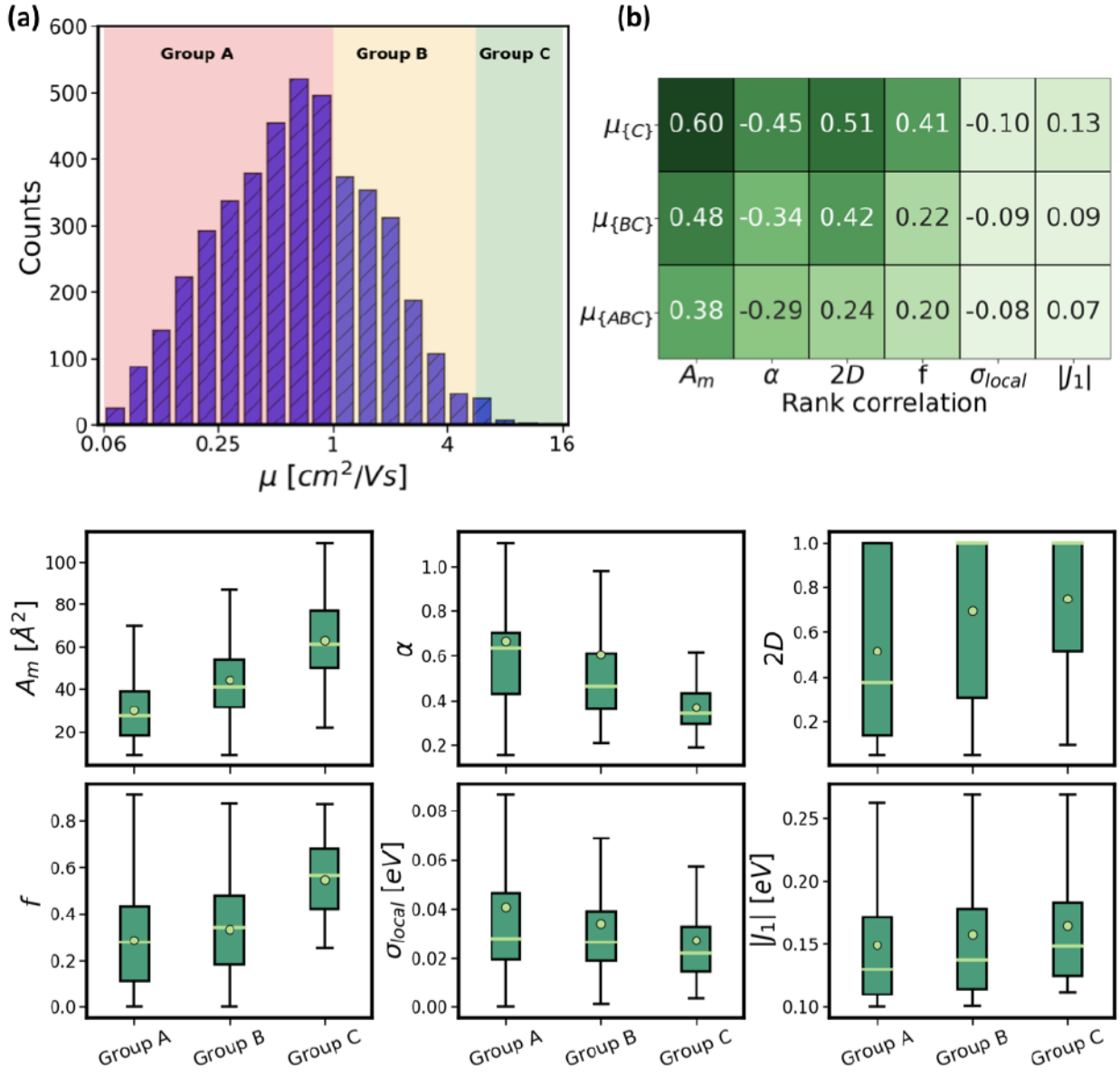

Figure 3. (a) Distribution of the computed mobility and separation of the materials into three groups (A, B, C) of increasing mobility. (b) The rank correlation matrix between the mobility and various parameters; {ABC} implies to the entire database, {BC} to structures only in groups B and C and finally {C} covers the top 40 molecules. (c) The variation range of system's parameters (A_m, α, $2D$, f, σ_{local}, $|J_1|$) among the different categories of mobility (groups A, B, C) depicted on a series of "box plots". The box limits represent the first (Q_1) and third quartiles (Q_3), with a line and a small circle representing the median and the mean value, respectively.

The analysis of the literature indicates that among the top 40 molecules in Group C, only 15 have been considered as high-mobility materials for transport, 10 appears in other optoelectronic/photonic applications, and 15 have never been considered as semiconducting materials. Evidently, such high throughput screening can directly suggest a few interesting avenues of investigation. In Figure 4(a), four representative molecules from each aforementioned categories are represented. In the SI (pages 12-13), the sketch of all the top 40 molecules is represented with a table (Table S1, page 11) containing the list of all the top 40 molecules (with a link to their CSD repository), their chemical formula, their frontier orbitals energies, their computed mobility and the bibliographic reference to the original synthetic work. One of the most interesting observations for the development of the field is that the best materials tend to be good or excellent in most but typically not all the desirable characteristics and the distribution of the key properties in the good and excellent materials is extremely broad. This is best explained in Figure 4(b), where a series of colour-coded tables illustrate how good each parameter is (when ranked from best to worse) for three groups of materials: all the high-mobility materials (group C) and a random selection of the intermediate and low computed mobility. The highest mobility materials have typically the best combination of properties but in no case, all the properties are in the optimal range. Moreover, the properties that are sub-optimal are different within the top 40 materials, i.e. there is no single reason why a high mobility material fails to be better. For instance, the crystal structure identified by “TUFMOY” (highlighted in Figure (4)) presents an undesirable molecular area, which is compensated by a particularly favourable electronic structure and small electron-phonon couplings. Similarly, the “CIYYAM” crystal (highlighted in Figure (4)) also manifests desirable charge mobility in spite of a weak electronic structure as the other parameters are in their ideal regime. These kinds of rationalizations enable one to explain why a particular material exhibits desirable/undesirable charge transport properties. The usefulness of this scheme for materials discovery is confirmed by the tables describing intermediate- and low-mobility materials where the reduction of the computed mobility is associated to a chequered degradation of all the parameters.

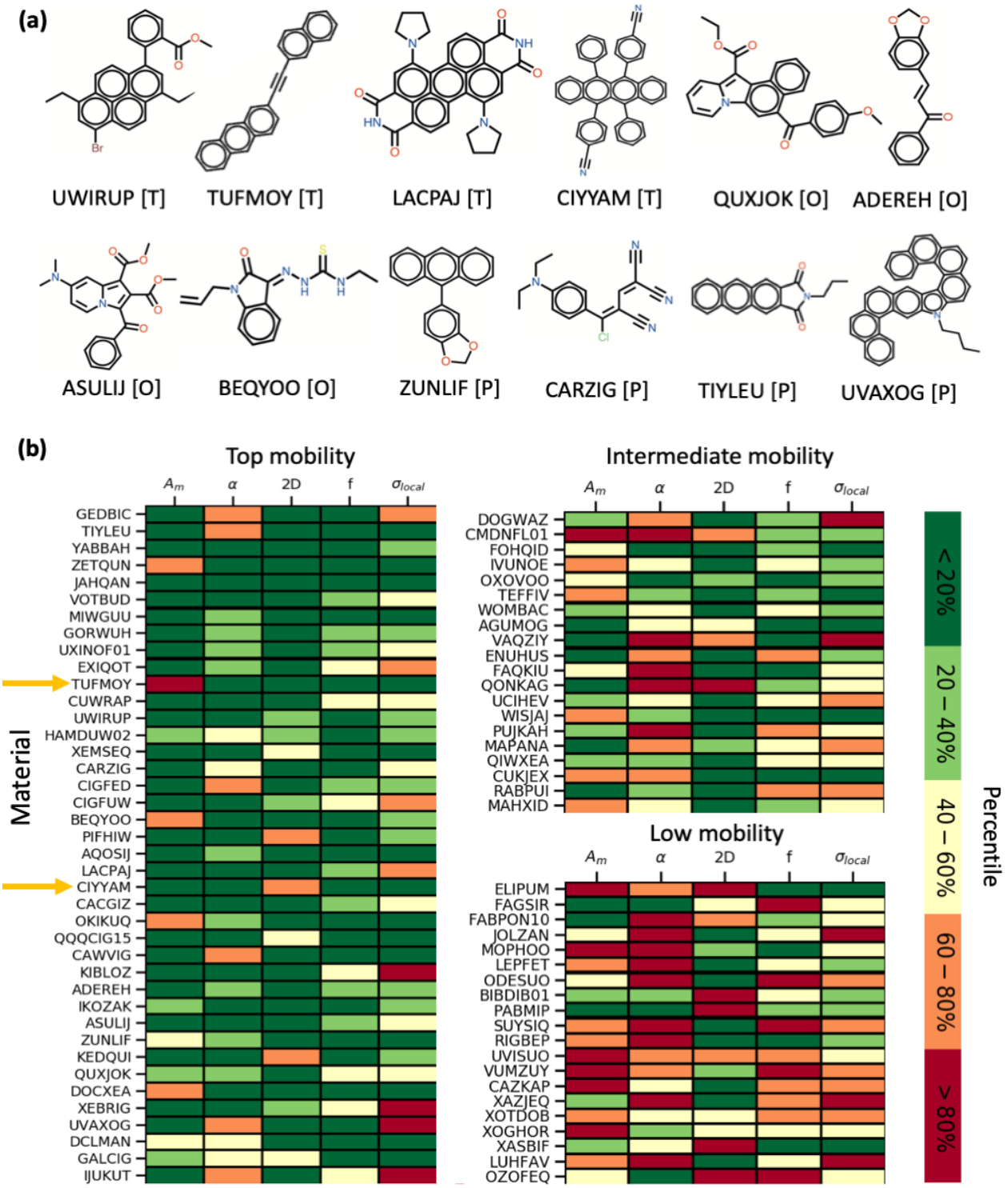

Figure 4. (a) A sample of high-mobility materials (selected from the top 40 molecules of group C) with their CSD identifiers. The letter given in brackets indicates the original purpose of molecule's synthesis ([T] charge transport, [P] photo-physical properties and [O] other applications). (b) Colour-coded table highlighting the position of the parameters for a set of high- (>6 cm^2/Vs), intermediate- (3-6 cm^2/Vs) and low- (0.9-1.2 cm^2/Vs) mobility materials in the entire database. The labels in the vertical axis represent the materials identifiers in the CSD. Chemical structure and link to the crystallographic structure are given in the SI (pages 11-13). Top materials are given in decreasing order of mobility.

The natural final step is to determine whether it is possible to optimize the materials further, i.e. if it is practical to improve *independently* the desirable characteristics and what mobility one can expect to achieve. Since, as illustrated previously, the main characteristics for high mobility are either uncorrelated or constructively correlated, one *can* imagine a gradual improvement of the performance based on improving each one of them. To understand what is feasible we observed that (Figure 5) a good but not outstanding mobility of 6 cm^2/Vs can be obtained with a hypothetical material where all the 5 important characteristics (i.e. A_m, α, $2D$, f and σ_{local}) have been chosen to be in the top 20 percentile. We can then "simulate" the hypothetical performance of a material whose characteristics are uniformly improved within the realistic range. Mobility of 12 cm^2/Vs is achieved if all characteristics are in the top 10 percentile and by setting them in the top 1 percentile the computed mobility is 70 cm^2/Vs, which can be seen as a realistic limit for this technology. The results of the computations can be used to identify suitable materials for in-depth investigation of mobility with alternative (and generally more expensive) methods. For example, if materials with mobility of few tens of cm^2/Vs are found a description in terms of band transport may become more desirable.[48]

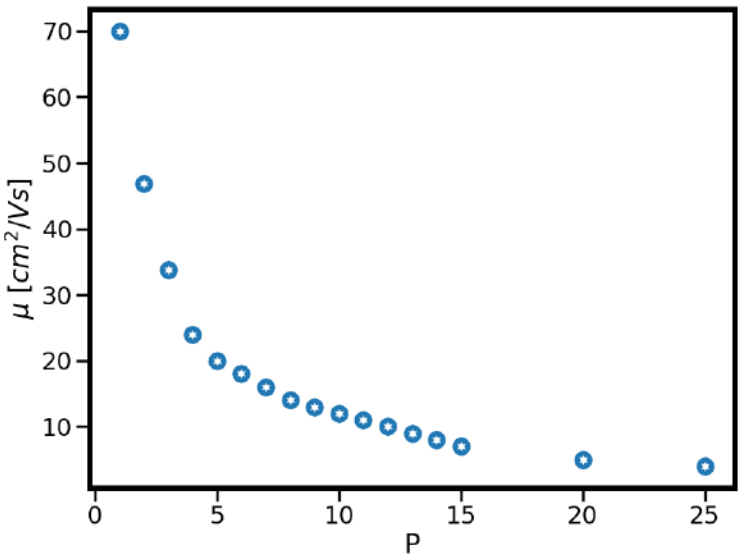

Figure 5. Expected mobility for a hypothetical material with all the important characteristics (A_m, α, $2D$, f and σ_{local}) selected to be simultaneously in the best P percentile of the distribution of real materials (details in the SI).

4. Conclusion

The work presented here provides (i) a new tool for discovery of new materials, (ii) a set of possible compounds to be investigated, and (iii) a possible strategy to identify better compounds. The new tool is the ability to perform an accurate evaluation of the mobility from the crystal structure in a fully automated procedure that takes just a few CPU hours. It can be used to identify promising materials to be purified

and optimized for device measurement after the first powder diffraction characterization. Furthermore, having demonstrated the ability to perform thousands of mobility evaluations, this tool can be coupled to crystal structure prediction (CSP) methods[57,58] to establish if, among the low energy compounds predicted by CSP, there are some with sufficient potential to justify the effort for the synthesis. For the first time, the rate-determining step for this prediction is the CSP rather than the mobility calculation and, for this reason, one can tolerate some degree of uncertainty still present in the prediction of crystal structures.

The exploration of the Cambridge Structural Database provided a good number of compounds never considered as high mobility materials that are expected to have high mobility, subject to the ability to produce single crystal highly purified devices from them. Possibly even more important is the mapping of the range of properties plausible and their likelihood for a statistically large sample. For example, it enables one to observe that there is scope to reduce substantially the non-local electron-phonon coupling, a fact only subject to speculation so far. The data allow one to find answers to many questions posed in the literature (how likely it is to make a three-dimensional semiconductor, what is the smallest effective mass that is reasonable, etc.). An important finding is that the properties contributing to the mobility are broadly uncorrelated, implying that one can possibly optimize them separately. This result is robust and independent of the model of transport adopted.

Further insight is obtained by correlating the computed mobility with the materials property. One finds that the best materials are far from being optimal with respect to all the properties and one can even identify the maximum achievable mobility using physically reasonable parameters. While this is subject to the theory used for the computation of the mobility the general principle can be used to determine the maximum achievable mobility according to any advanced method to be developed. Given the relative importance of these parameters, we note that a good degree of rational bottom-up design is possible without resorting the crystal structure prediction. The molecular parameters f and σ_{local} can be computed with great accuracy for many hypothetical molecules before their synthesis and sub-optimal molecules excluded in that phase.[59] Crystal engineering, where an approximated structure can be predicted by exploiting the modification of known structures, can be used to control the molecular area and at least avoid one-dimensional stacks, leaving the strength of transfer integral fluctuations as the only property we have insignificant control over. In this way, having reduced the search space and identified the achievable optimum we can increase the success rate of trial and error approaches.

DATA AVAILABILITY. Electronic supplementary information (SI) available: details on the (i) effective Hamiltonian; (ii) transfer integrals calculations; (iii) local electron-phonon coupling; (iv) non-local electron-phonon coupling and check of approximations; (v) mobility calculations in the framework of transient

localization theory; (vi) largest plausible mobility; (vii) computational time and (viii) electronic structure/crystallographic information of the top 40 molecules, their molecular diagrams and also the sketch of 6 materials identified as three-dimensional structures. In addition, we provide public access to the list of 40 k materials identified as semiconductors in this work, to the two highest transfer integrals (J_1 and J_2) for all the 40 k structures and to all the raw data utilized in colour-coded tables in Figure (4).

ACKNOWLEDGMENTS. This work was supported by ERC-PoC grant (Grant 403098).

REFERENCES:

[1] S. Curtarolo, G. L. W. Hart, M. B. Nardelli, N. Mingo, S. Sanvito, O. Levy, *Nat. Mater.* **2013**, *12*, 191.
[2] R. Gómez-Bombarelli, J. Aguilera-Iparraguirre, T. D. Hirzel, D. Duvenaud, D. Maclaurin, M. A. Blood-Forsythe, H. S. Chae, M. Einzinger, D.-G. Ha, T. Wu, G. Markopoulos, S. Jeon, H. Kang, H. Miyazaki, M. Numata, S. Kim, W. Huang, S. I. Hong, M. Baldo, R. P. Adams, A. Aspuru-Guzik, *Nat. Mater.* **2016**, *15*, 1120.
[3] E. O. Pyzer-Knapp, C. Suh, R. Gómez-Bombarelli, J. Aguilera-Iparraguirre, A. Aspuru-Guzik, *Annu. Rev. Mater. Res.* **2015**, *45*, 195.
[4] N. R. Goud, X. Zhang, J.-L. Brédas, V. Coropceanu, A. J. Matzger, *Chem* **2018**, *4*, 150.
[5] K. T. Butler, J. M. Frost, J. M. Skelton, K. L. Svane, A. Walsh, *Chem. Soc. Rev.* **2016**, *45*, 6138.
[6] R. J. Maurer, C. Freysoldt, A. M. Reilly, J. G. Brandenburg, O. T. Hofmann, T. Björkman, S. Lebègue, A. Tkatchenko, *Annu. Rev. Mater. Res.* **2019**, *49*, 1.
[7] D. Padula, Ö. H. Omar, T. Nematiaram, A. Troisi, *Energy Environ. Sci.* **2019**, *12*, 2412.
[8] M. C. Hanna, A. J. Nozik, *J. Appl. Phys.* **2006**, *100*, 074510.
[9] A. Kuzmich, D. Padula, H. Ma, A. Troisi, *Energy Environ. Sci.* **2017**, *10*, 395.
[10] V. Stanev, C. Oses, A. G. Kusne, E. Rodriguez, J. Paglione, S. Curtarolo, I. Takeuchi, *npj Comput. Mater.* **2018**, *4*, 29.
[11] C. Schober, K. Reuter, H. Oberhofer, *J. Phys. Chem. Lett.* **2016**, *7*, 3973.
[12] R. Li, X. Li, L. Xi, J. Yang, D. J. Singh, W. Zhang, *ACS Appl. Mater. Interfaces* **2019**, *11*, 24859.
[13] J. L. Brédas, J. E. Norton, J. Cornil, V. Coropceanu, *Acc. Chem. Res.* **2009**, *42*, 1691.
[14] J.-L. Brédas, D. Beljonne, V. Coropceanu, J. Cornil, *Chem. Rev.* **2004**, *104*, 4971.
[15] G. Schweicher, G. Garbay, R. Jouclas, F. Vibert, F. Devaux, Y. H. Geerts, *Adv. Mater.* **2020**, *1905909*, 1905909.
[16] H. H. Choi, K. Cho, C. D. Frisbie, H. Sirringhaus, V. Podzorov, *Nat. Mater.* **2017**, *17*, 2.
[17] O. D. Jurchescu, J. Baas, T. T. M. Palstra, *Appl. Phys. Lett.* **2004**, *84*, 3061.
[18] G. Horowitz, M. E. Hajlaoui, R. Hajlaoui, *J. Appl. Phys.* **2000**, *87*, 4456.
[19] W. Xie, K. A. McGarry, F. Liu, Y. Wu, P. P. Ruden, C. J. Douglas, C. D. Frisbie, *J. Phys. Chem. C* **2013**, *117*, 11522.
[20] V. Podzorov, V. M. Pudalov, M. E. Gershenson, *Appl. Phys. Lett.* **2003**, *82*, 1739.
[21] V. Podzorov, E. Menard, J. A. Rogers, M. E. Gershenson, *Phys. Rev. Lett.* **2005**, *95*, 226601.
[22] N. A. Minder, S. Ono, Z. Chen, A. Facchetti, A. F. Morpurgo, *Adv. Mater.* **2012**, *24*, 503.
[23] S. Fratini, D. Mayou, S. Ciuchi, *Adv. Funct. Mater.* **2016**, *26*, 2292.
[24] H. Oberhofer, K. Reuter, J. Blumberger, *Chem. Rev.* **2017**, *117*, 10319.
[25] V. Coropceanu, J. Cornil, D. A. da Silva Filho, Y. Olivier, R. Silbey, J. L. Brédas, *Chem. Rev.* **2007**, *107*, 926.
[26] NOTE: The electron-phonon coupling terms in this manuscript are the leading ones proportional to the displacement – there could be higher order terms.
[27] A. Troisi, *Org. Electron.* **2011**, *12*, 1988.
[28] T. F. Harrelson, V. Dantanarayana, X. Xie, C. Koshnick, D. Nai, R. Fair, S. A. Nuñez, A. K. Thomas, T. L. Murrey, M. A. Hickner, J. K. Grey, J. E. Anthony, E. D. Gomez, A. Troisi, R. Faller, A. J. Moulé, *Mater. Horizons* **2019**, *6*, 182.
[29] A. Troisi, G. Orlandi, J. E. Anthony, *Chem. Mater.* **2005**, *17*, 5024.
[30] J. L. Bredas, J. P. Calbert, D. A. da Silva Filho, J. Cornil, *Proc. Natl. Acad. Sci.* **2002**, *99*, 5804.
[31] L. Wang, O. V. Prezhdo, D. Beljonne, *Phys. Chem. Chem. Phys.* **2015**, *17*, 12395.

[32] S. Fratini, S. Ciuchi, D. Mayou, G. T. de Laissardière, A. Troisi, *Nat. Mater.* **2017**, *16*, 998.

[33] S. Giannini, A. Carof, M. Ellis, H. Yang, O. G. Ziogos, S. Ghosh, J. Blumberger, *Nat. Commun.* **2019**, *10*, 3843.

[34] G. Schweicher, G. D'Avino, M. T. Ruggiero, D. J. Harkin, K. Broch, D. Venkateshvaran, G. Liu, A. Richard, C. Ruzié, J. Armstrong, A. R. Kennedy, K. Shankland, K. Takimiya, Y. H. Geerts, J. A. Zeitler, S. Fratini, H. Sirringhaus, *Adv. Mater.* **2019**, *31*, 1902407.

[35] N.-E. Lee, J.-J. Zhou, L. A. Agapito, M. Bernardi, *Phys. Rev. B* **2018**, *97*, 115203.

[36] X. Xie, A. Santana-bonilla, A. Troisi, *J. Chem. Theory Comput.* **2018**, *14*, 3752.

[37] N. Bedoya-Martínez, A. Giunchi, T. Salzillo, E. Venuti, R. G. Della Valle, E. Zojer, *J. Chem. Theory Comput.* **2018**, *14*, 4380.

[38] T. F. Harrelson, V. Dantanarayana, X. Xie, C. Koshnick, D. Nai, R. Fair, S. A. Nuñez, A. K. Thomas, T. L. Murrey, M. A. Hickner, J. K. Grey, J. E. Anthony, E. D. Gomez, A. Troisi, R. Faller, A. J. Moulé, *Mater. Horizons* **2019**, *6*, 182.

[39] A. Landi, A. Troisi, *J. Phys. Chem. C* **2018**, *122*, 18336.

[40] C. R. Groom, I. J. Bruno, M. P. Lightfoot, S. C. Ward, *Acta Crystallogr. Sect. B Struct. Sci. Cryst. Eng. Mater.* **2016**, *72*, 171.

[41] A. Troisi, G. Orlandi, *Chem. Phys. Lett.* **2001**, *344*, 509.

[42] S. S. Batsanov, *Inorg. Mater.* **2001**, *37*, 871.

[43] J. E. Norton, J.-L. Brédas, *J. Am. Chem. Soc.* **2008**, *130*, 12377.

[44] L. W. Chung, W. M. C. Sameera, R. Ramozzi, A. J. Page, M. Hatanaka, G. P. Petrova, T. V. Harris, X. Li, Z. Ke, F. Liu, H.-B. Li, L. Ding, K. Morokuma, *Chem. Rev.* **2015**, *115*, 5678.

[45] M. J. Frisch, G. W. Trucks, H. B. Schlegel, others, *Gaussian Inc., Wallingford CT* **2016**.

[46] M. Malagoli, V. Coropceanu, D. A. da Silva Filho, J. L. Brédas, *J. Chem. Phys.* **2004**, *120*, 7490.

[47] S. Ciuchi, S. Fratini, D. Mayou, *Phys. Rev. B* **2011**, *83*, 081202.

[48] S. Fratini, S. Ciuchi, *Phys. Rev. Res.* **2020**, *2*, 013001.

[49] T. Nematiaram, S. Ciuchi, X. Xie, S. Fratini, A. Troisi, *J. Phys. Chem. C* **2019**, *123*, 6989.

[50] A. Landi, *J. Phys. Chem. C* **2019**, *123*, 18804.

[51] B. Blülle, A. Troisi, R. Häusermann, B. Batlogg, *Phys. Rev. B* **2016**, *93*, 035205.

[52] A. Landi, R. Borrelli, A. Capobianco, A. Velardo, A. Peluso, *J. Phys. Chem. C* **2018**, *122*, 25849.

[53] J. Kirkpatrick, V. Marcon, J. Nelson, K. Kremer, D. Andrienko, *Phys. Rev. Lett.* **2007**, *98*, 1.

[54] T. Kubo, R. Häusermann, J. Tsurumi, J. Soeda, Y. Okada, Y. Yamashita, N. Akamatsu, A. Shishido, C. Mitsui, T. Okamoto, S. Yanagisawa, H. Matsui, J. Takeya, *Nat. Commun.* **2016**, *7*, 11156.

[55] K. Hannewald, V. M. Stojanović, J. M. T. Schellekens, P. A. Bobbert, G. Kresse, J. Hafner, *Phys. Rev. B* **2004**, *69*, 075211.

[56] L. Wang, D. Beljonne, *J. Phys. Chem. Lett.* **2013**, *4*, 1888.

[57] P. Cui, D. P. McMahon, P. R. Spackman, B. M. Alston, M. A. Little, G. M. Day, A. I. Cooper, *Chem. Sci.* **2019**, *10*, 9988.

[58] A. M. Reilly, R. I. Cooper, C. S. Adjiman, S. Bhattacharya, A. D. Boese, J. G. Brandenburg, P. J. Bygrave, R. Bylsma, J. E. Campbell, R. Car, D. H. Case, R. Chadha, J. C. Cole, K. Cosburn, H. M. Cuppen, F. Curtis, G. M. Day, R. A. DiStasio Jr, A. Dzyabchenko, B. P. van Eijck, D. M. Elking, J. A. van den Ende, J. C. Facelli, M. B. Ferraro, L. Fusti-Molnar, C.-A. Gatsiou, T. S. Gee, R. de Gelder, L. M. Ghiringhelli, H. Goto, S. Grimme, R. Guo, D. W. M. Hofmann, J. Hoja, R. K. Hylton, L. Iuzzolino, W. Jankiewicz, D. T. de Jong, J. Kendrick, N. J. J. de Klerk, H.-Y. Ko, L. N. Kuleshova, X. Li, S. Lohani, F. J. J. Leusen, A. M. Lund, J. Lv, Y. Ma, N. Marom, A. E. Masunov, P. McCabe, D. P. McMahon, H. Meekes, M. P. Metz, A. J. Misquitta, S. Mohamed, B. Monserrat, R. J. Needs, M. A. Neumann, J. Nyman, S. Obata, H. Oberhofer, A. R. Oganov, A. M. Orendt, G. I. Pagola, C. C. Pantelides, C. J. Pickard, R. Podeszwa, L. S. Price, S. L. Price, A. Pulido, M. G. Read, K. Reuter, E. Schneider, C. Schober, G. P. Shields, P. Singh, I. J. Sugden, K. Szalewicz, C. R. Taylor, A. Tkatchenko, M. E. Tuckerman, F. Vacarro, M. Vasileiadis, A. Vazquez-Mayagoitia, L. Vogt, Y. Wang, R. E. Watson, G. A. de Wijs, J. Yang, Q. Zhu, C. R. Groom, *Acta Crystallogr. Sect. B Struct. Sci. Cryst. Eng. Mater.* **2016**, *72*, 439.

[59] V. Coropceanu, R. S. Sánchez-Carrera, P. Paramonov, G. M. Day, J. L. Brédas, *J. Phys. Chem. C* **2009**, *113*, 4679.